inorganics

MDPI

Article

Extended Synthetic Pathways Towards Dialkyl-Substituted Phosphanylboranes

Mehdi Elsayed Moussa †, Oliver Hegen †, Christoph Riesinger and Manfred Scheer *

Department of Inorganic Chemistry, University of Regensburg, 93040 Regensburg, Germany; mehdi.elsayed-mousa@chemie.uni-regensburg.de (M.E.M.); oliver.hegen@chemie.uni-regensburg.de (O.H.); christoph.riesinger@chemie.uni-regensburg.de (C.R.)

* Correspondence: manfred.scheer@ur.de; Tel.: +49-(0)941-943-4440; Fax: +49-(0)941-943-4439

† These authors contributed equally to this work.

Abstract

Phosphine–boranes have garnered growing interest for their potential in catalysis and as building blocks for inorganic polymers. While various synthetic methods exist, flexibility to introduce diverse substituents on the P centers remains limited. Our group reported routes to monoalkylated phosphanylboranes starting from primary phosphanylboranes or sodium phosphide. In this work, we extend these strategies to enable the synthesis of dialkylated phosphanylboranes bearing either identical or different substituents on the P atoms. This expanded methodology provides access to a broader scope of diverse P centers, a key factor influencing the reactivity and applications of phosphine–borane derivatives.

Keywords: alkylation; boron; phosphanylboranes; phosphonium salts; phosphorus

1. Introduction

In the last two decades, an increasing interest has been witnessed in the synthesis and reactivity study of phosphine–borane compounds, particularly due to their potential as starting materials for the synthesis of inorganic polymers through dehydrocoupling reactions [1–4]. Given that P−B bonds are isoelectronic with C−C single bonds, poly(phosphine–boranes) are considered an alternative class of inorganic analogs to organic polymers, such as polyolefins, albeit with significantly different properties [5–10]. Phosphine–borane monomers are also highly versatile molecules. They have been widely employed in synthesis and catalysis [11–22] and, to a lesser extent, in biomedical applications [23–25], as well as in the activation and transfer of H_2 and other small molecules [26–30]. Interestingly, these compounds are easily accessible, highly modular, and offer valuable insights via multi-nuclear NMR spectroscopy. Over time, a number of methods have been developed for the synthesis of these compounds. Typical approaches involve the reaction of phosphines (PR_3, R = H, alkyl, aryl) with diboranes, borane complexes, or borohydrides [31]. Alternatively, chlorophosphines can be reduced with sodium or lithium borohydrides to avoid the use of primary and secondary phosphines, which are often challenging to handle [13,31]. Additionally, a number of secondary and tertiary phosphine–boranes have been prepared from direct reduction of phosphine oxides [31–33]. One of our group's contributions to this field involves the synthesis and reactivity of Lewis base-stabilized pnictogenylboranes $R_2E\text{-}BH_3{\bullet}NMe_3$ (E = P, As; R = H, alkyl, aryl) [34,35]. Consequently, their coordination [36], oxidation [37], oligomerization [38], and polymerization [39] chemistry have been investigated. Moreover, these compounds have been

check for updates

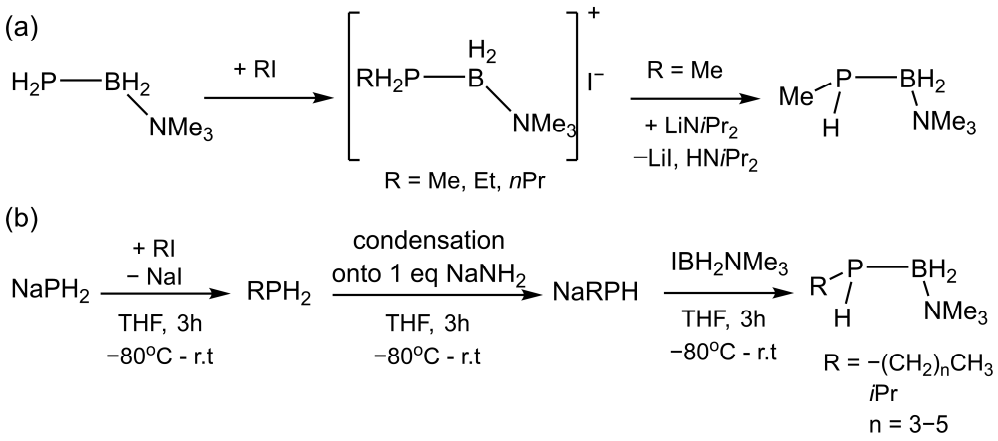
Academic Editors: Axel Klein and Hicham Idriss

Received: 18 June 2025
Revised: 2 July 2025
Accepted: 8 July 2025
Published: 11 July 2025

Citation: Moussa, M.E.; Hegen, O.; Riesinger, C.; Scheer, M. Extended Synthetic Pathways Towards Dialkyl-Substituted Phosphanylboranes. *Inorganics* **2025**, *13*, 239. https://doi.org/10.3390/inorganics13070239

Copyright: © 2025 by the authors. Licensee MDPI, Basel, Switzerland. This article is an open access article distributed under the terms and conditions of the Creative Commons Attribution (CC BY) license (https://creativecommons.org/licenses/by/4.0/).

utilized in the synthesis of cationic and anionic chain compounds, built up by R_2P-BH_2 units [40,41]. Considering that even minor modifications of the substituents on the P or B atoms can significantly impact the reactivity of phosphanylborane [42,43], we have become highly interested in developing new routes to facilitate such modifications. Accordingly, we created a straightforward route to high-yield mono-alkylated phosphonium iodides, [RPH_2-BH_2•NMe_3]I (R = Me, Et, *n*Pr; Scheme 1a), from the reaction of iodoalkanes with PH_2-BH_2•NMe_3. The methyl phosphonium iodide was further treated with lithium diisopropylamide, yielding the methyl-substituted phosphanylborane (HMeP-BH_2•NMe_3), which was subsequently used as a precursor to poly(methylphosphanylborane) via simple thermolysis [44]. More recently, another more general method was developed. This method involves the synthesis of mono-alkylated phosphines from $NaPH_2$ and iodoalkanes, followed by a one-pot metalation of the phosphine by $NaNH_2$. Finally, a salt metathesis of the resulting phosphanide NaRHP with IBH_2NMe_3 yields the targeted mono-P-substituted phosphanylboranes in good yields and on a gram scale (Scheme 1b) [45].



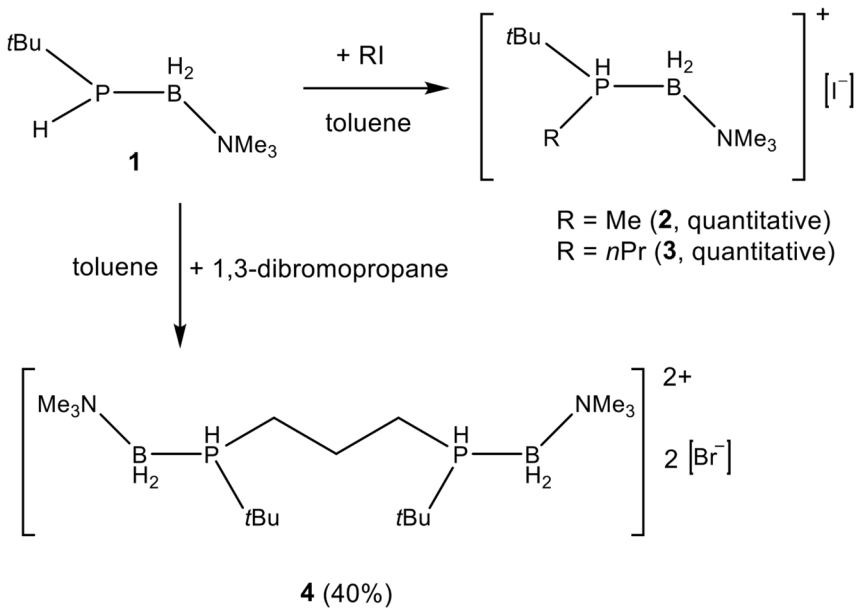
Scheme 1. Two approaches recently reported towards the synthesis of mono-alkyl-substituted phosphanylboranes. (**a**) Synthesis of mono-alkylated phosphonium salts and methylphosphanylborane; (**b**) General route for the synthesis of mono-alkyl-substituted phosphanylboranes via salt metathesis of mono-alkylated phosphines.

In view of these results, the question arises whether it is possible to broaden the scope of these methods towards dialkylated phosphanylboranes, especially with two different substituents on the P atoms. Herein, we report the extension of our first method towards dialkyl-substituted phosphanylborane derivatives (RR'PH_2-BH_2•NMe_3) proceeding via phosphonium iodide intermediates. In addition, we adapted the salt metathesis step of our second approach to access similar disubstituted compounds. The first method, which involves a stepwise alkylation pathway from primary to tertiary phosphanylboranes, provides flexibility in introducing different substituents on the P atom, allowing for the formation of unprotected chiral phosphanylboranes, which are not accessible by other reported methods in the field. While herein these species are obtained as racemic mixtures, related phosphanylboranes could be prepared enantiomerically pure, which holds promise for future investigations [46–50].

2. Results and Discussion

To demonstrate the feasibility of our reported methods toward new dialkylated phosphanylboranes, we selected, in a first approach, the secondary phosphanylborane *t*BuPH$BH_2$$NMe_3$ (**1**) [39] and reacted it with alkyl halides (MeI; *n*PrI; 1,3-dibrompropane). These reactions were carried out in toluene by stirring the reaction mixture for 20 h at room temperature. After evaporation of the solvents, white solids of the corresponding

alkylated phosphonium salts (*t*Bu(Me)PHBH$_2$NMe$_3$)I (**2**), (*t*Bu(*n*Pr)PHBH$_2$NMe$_3$)I (**3**), and [{(Me$_3$NH$_2$BHP*t*Bu)*n*Pr(*t*BuPHBH$_2$NMe$_3$)}(Br)$_2$] (**4**), respectively, were obtained (Scheme 2) after washing them with *n*-hexane (**2**, **3**) or toluene (**4**) to remove any traces of the used alkyl halides. Based on their ^{31}P NMR spectra, elemental analysis, and the weight of the isolated powders, compounds **2** and **3** were formed selectively and in quantitative yields.



Scheme 2. Syntheses of compounds **2**–**4** (yields are given in parenthesis).

However, the ^{31}P and ^{11}B NMR spectra of the crude reaction mixture of **4** revealed unidentified side products, reducing its yield to about 40%. Compounds **2**–**4** are highly soluble in common organic solvents, including *n*-alkanes. Their ^{31}P NMR spectra show signals centered at −15.7, −7.4, and −10.4 ppm, respectively, all of which are downfield-shifted compared to the phosphanylborane salt **1** (−67.6 ppm) [39]. However, in the ^{11}B NMR spectra, the signals attributed to the BH$_2$-moiety (−10.3 (**2**), −11.1 (**3**), and −10.9 (**4**) ppm) are found upfield-shifted compared to that of **1** (−6.0 ppm, Table 1) [39]. In the ESI-MS spectra recorded in CD$_3$CN, molecular ion peaks were observed in the positive ion mode for all the products **2**–**4**. Additionally, peaks attributed to the cations [(**3**)$_2$(I)]$^+$ and [(**4**)(Br)]$^+$ were detected for **3** and **4**, respectively.

Table 1. NMR data for the phosphonium halides **1**–**4** at 300 K.

	δ [ppm] (*J* [Hz])				
	^{1}H			^{31}P	^{11}B
	PH ($^1J_{PH}$)	BH$_2$ ($^1J_{BH}$)	N(CH$_3$)$_3$	P*t*BuR ($^1J_{PB}$)	BH$_2$
1	2.60 (197)	2.67 (104)	1.94	−67.6 (48)	−6.0
2	5.47 (396)	2.15 (113)	2.83	−15.7 (78)	−10.3
3	5.29 (380)	2.40 (110)	2.81	−7.4 (73)	−11.1
4	6.41 (390)	2.27–2.61	2.89	−10.4 (70)	−10.9

Single crystals of compounds **2**–**4** were obtained by layering their THF/MeCN (**2**, **3**) or CH$_2$Cl$_2$ (**4**) solutions with *n*-hexane. Their molecular structures in the solid state were determined by single crystal X-ray diffraction analysis (Figure 1). Compound **2** crystallizes in the monoclinic space group $P2_1/n$, compound **3** in the triclinic space group $P\bar{1}$, and compound **4** in the orthorhombic space group $Pna2_1$. The unit cells of **2** and **3** contain both

the R and the S enantiomers of the respective compound, whereas only the meso-form of **4** is observed in its unit cell. All bond lengths in **2**–**4** are consistent with single bonds.

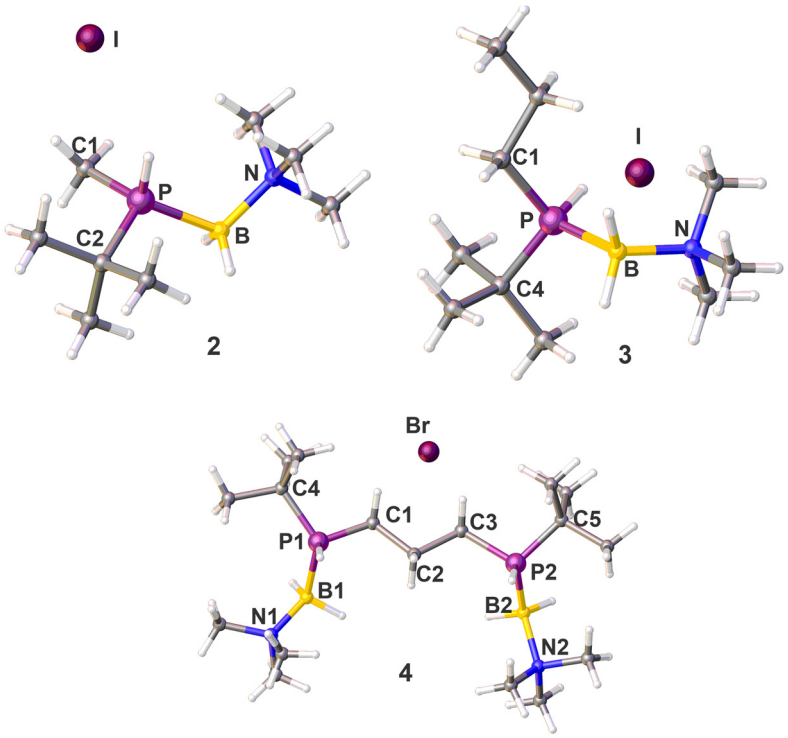


Figure 1. Molecular structures of the phosphanylborane salts **2**–**4** in the solid state.

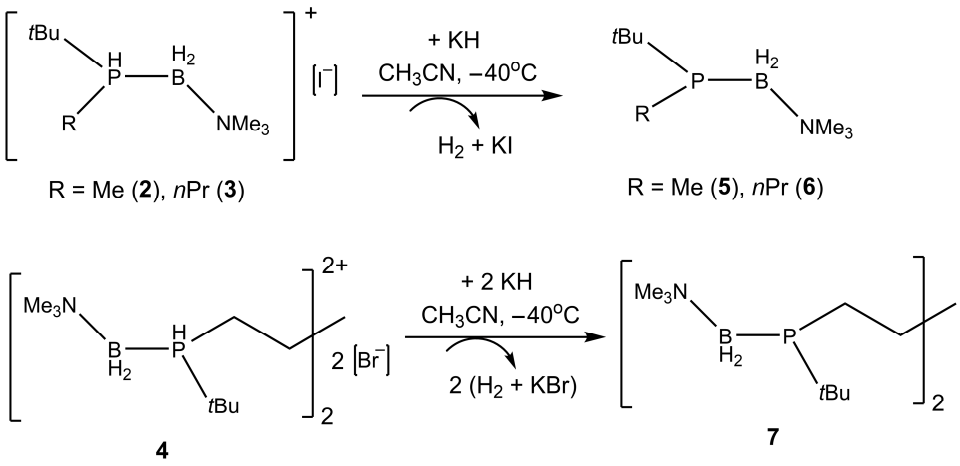
The B–P (**2**: 1.968(5) Å, **3**: 1.956(6)/1.966(5)Å, **4**: 1.90(5)/2.01(2) Å) and B–N (**2**: 1.594(5) Å, **3**: 1.599(7)/1.602(8) Å, **4**: 1.55(3)/1.69(4) Å) bond lengths in **2**–**4** are similar to those observed for **1** (1.985(2) and 1.621(2) Å, respectively) [42]. The P atoms in compounds **2**–**4** exhibit slightly disordered tetrahedral environments, with each connected to two C atoms, one H atom, and one B atom (Table 2). In both **2** and **3**, the B–P axis shows an antiperiplanar arrangement, whereas it shows an anticlinal arrangement in **4**.

Table 2. Selected bond distances [Å] and angles [°] for compounds **1**–**4**.

Compound	1	2	3	4
P−B	1.985(2)	1.968(5)	1.956(6)–1.966(5)	1.90(2)–2.01(2)
B−N	1.621(2)	1.594(5)	1.599(7)–1.602(8)	1.55(3)–1.69(4)
P−C	1.890(2)	1.804(5)–1.832(4)	1.818(5)–1.863(5)	1.72(2)–1.86(2)
P−B−N	108.9(1)	112.4(3)	114.0(3)–115.4(3)	116.9(2)–118.2(2)
C−P−C	-	109.7(2)	108.7(2)–109.2(2)	102.8(1)–106.5(9)

Deprotonation of **2**–**4** with KH in CH_3CN leads to the dialkylated neutral phosphanylboranes *t*BuPRBH_2NMe_3 (R = Me(**5**), *n*Pr (**6**)) and [(Me$_3$NBH_2P*t*Bu)$_2$*n*Pr] (**7**), respectively (Scheme 3). According to the ^{11}B and ^{31}P NMR spectroscopy, all the reactions proceeded to completion. However, minor impurities were still present after extracting the products with *n*-hexane due to the very good solubility of trace impurities and **5**–**7** in common organic solvents, including *n*-alkanes. Only compound **5** could be crystallized and, consequently, purely isolated in good yields (55%). In the ^{31}P NMR spectra of **5**–**7**, the signals of the P atoms (−53.38, −36.18 and −39.27 ppm, respectively) are upfield-shifted compared to those of **2**–**4**. In contrast, the resonances of the B atoms in the ^{11}B NMR spectra are downfield-

shifted (δ = −1.58 (**5**), −2.40 (**6**), and −2.73 (**7**) ppm) as compared to those observed for **2**–**4**.



Scheme 3. Syntheses of compounds **5**–**7**.

As expected, the molecular structure of **5** in the solid state (Figure 2) reveals a neutral compound with the absence of the proton on the P center and the I^- counterion. The P atom remains chiral, as it is bonded to three different groups and possesses a lone pair of electrons, but both enantiomers are found within the unit cell in the form of a 50:50 disorder. Similar to **2**, an antiperiplanar arrangement along the B–P bond is observed in **5**. The P–B bond length in **5** (2.002(2) Å) reveals a single bond and is slightly elongated compared to those found in **2** (1.969(5)/1.953(5) Å).

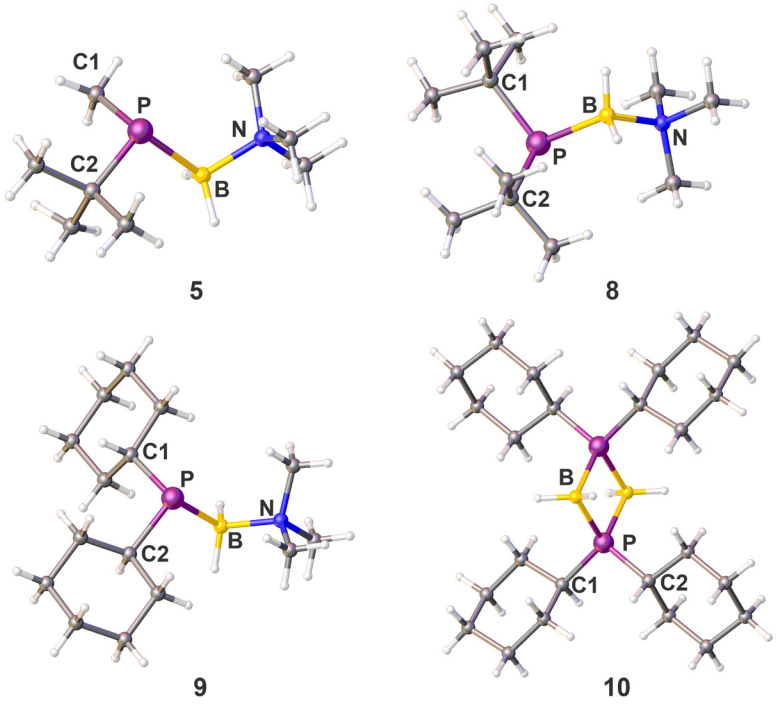
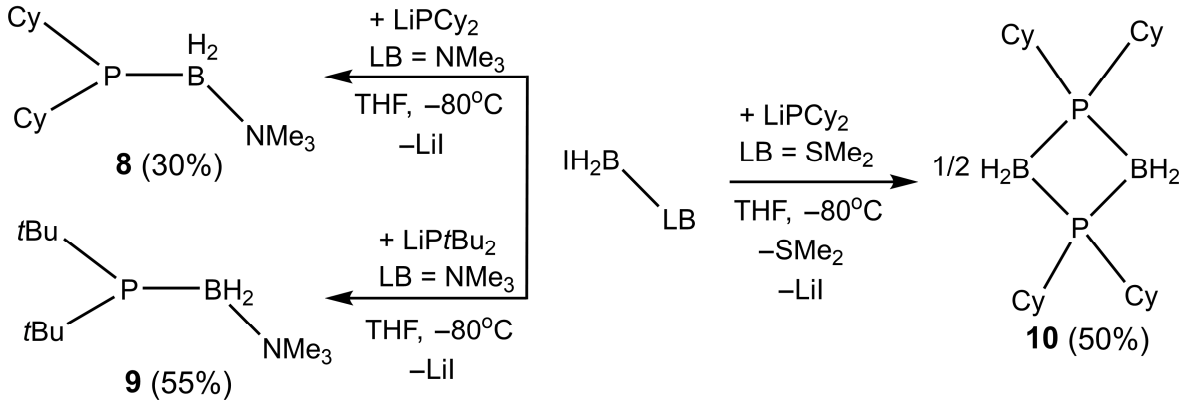


Figure 2. Molecular structures of **5** (**top left**), **8** (**top right**), **9** (**bottom left**), and **10** (**bottom right**) in the solid state.

In a second approach, the reaction of IBH_2NMe_3 with $LiPCy_2$ (Cy = cyclohexyl) and $LiPtBu_2$ [51], respectively, was investigated in THF at −80 °C. This reaction yielded the Lewis base (LB) stabilized dialkylated phosphanylboranes $Cy_2PBH_2NMe_3$ (**8**) and

*t*Bu$_2$PBH$_2$NMe$_3$ (**9**), respectively (Scheme 4). The synthesis of **8** and **9** proceeded to completion as revealed by the crude ^{31}P NMR spectra. However, the corresponding phosphines, HPCy$_2$ and HP*t*Bu$_2$, respectively, could be identified as side products. Thus, yields of 55% and 30%, respectively, were estimated for **8** and **9** based on the comparison of the integrals of the signals with side products. Due to the similar solubility of **8**/**9** and the phosphines, it was not possible to analytically isolate pure compounds.



Scheme 4. Syntheses of compounds **8**–**10**. Isolated yields are given in parenthesis.

Nevertheless, both compounds were characterized by single crystal X-ray diffraction analysis (Figure 2). They present an anticlinal arrangement along the P–B axis with ◁(N-B–P) = 111.00(16)° and 111.72(17)° and ◁(C1-P-C2) = 102.52(10)° and 109.952°, respectively. Additionally, their P–B (1.983(3) and 1.987(3) Å, respectively) and the B–N (1.645(3) and 1.636(4) Å, respectively) bond lengths are quite similar. The reaction of IBH$_2$SMe$_2$ with LiPCy$_2$ under similar reaction conditions yields the cyclic phosphanylborane (Cy$_2$PBH$_2$)$_2$ (**10**) featuring a four-membered ring motif in moderate yields (50%). The reaction probably includes the formation of Cy$_2$PBH$_2$SMe$_2$ as an intermediate, which undergoes dimerization and elimination of the weak LB SMe$_2$.

In contrast to **8** and **9**, compound **10** can be purely isolated, as it is not soluble in *n*-alkanes and thus can be separated from any impurities present in the crude reaction mixture. The resonance signals of the B and P nuclei are broad in both the ^{11}B and ^{31}P NMR spectra of **10**. Its ^{31}P{^{1}H} NMR spectrum at room temperature reveals a signal at $\delta = -10.88$ ppm ($\omega_{1/2}$ = 483 Hz), which is further broadened in its ^{31}P NMR spectrum ($\omega_{1/2}$ = 530 Hz). In the ^{11}B NMR spectrum, the signal of the B atoms ($\delta = -32.57$ ppm) is observed in the typical range of oligomeric or polymeric compounds [52]. In the ^{1}H NMR spectrum of **10**, signals of the cyclohexyl substituents appear at δ = 1.06–2.36 ppm and those of the BH$_2$ moieties at δ = 1.90 ppm as a broad multiplet. The molecular structure of **10** was determined by single crystal X-ray diffraction analysis (Figure 2). The P–B bond distance (1.9874(16) Å) corresponds to a P–B single bond. The slightly distorted square-planar conformation shows a P–B–P angle of ◁(P–B–P) = 88.144° and a B–P–B angle of ◁(B–P–B) = 91.856°. The P···P (2.766 Å) and the B···B (2.858 Å) distances are below the van der Waals radii (Σ r(P)vdW = 3.60 Å; r(B)vdW = 3.84 Å) [53]. In addition, irradiation of **10**, whether as a solid or in solution, with UV light (λ = 366 nm) shows visible blue luminescence. Emission measurements will be conducted in the near future to obtain further insights into the electronic properties of **10**, thus opening the door for a possible unexplored area of application for this class of compounds. It is worth mentioning that all compounds **1**–**10** are air- and moisture-sensitive, and their solids can only be stored for extended periods under an inert atmosphere, such as in a Schlenk tube or a glovebox.

3. Materials and Methods

3.1. General Information

All the manipulations were carried out under a dry argon or dinitrogen atmosphere using glovebox or standard Schlenk techniques. The solvents were taken from a solvent purification system of the MB-SPS-800 type from the company MBRAUN (Garching, Germany) and degassed by standard procedures. The starting materials, *t*BuPHBH$_2$NMe$_3$ [39], LiPCy$_2$ [51], Li*t*Bu$_2$P [51], IBH$_2$NMe$_3$ [41], and IBH$_2$SMe$_2$ [41], were prepared according to procedures outlined in the literature. The compounds MeI, *n*PrI, C$_3$H$_6$Br$_2$, and KH were purchased from the commercial suppliers Sigma-Aldrich Chemie GmbH (Eschenstraße 5, 82024 Taufkirchen, Germany), Thermo Fisher Scientific GmbH (Im Steingrund 4-6, 63303 Dreieich, Germany), and Merck Chemicals GmbH (Frankfurter Straße 133, 64293 Darmstadt, Germany), respectively. All the nuclear magnetic resonance (NMR) spectra were recorded on a Bruker Avance 400 spectrometer (Brucker Instruments, Ettlingen, Germany) (^{1}H: 400.13 MHz, ^{31}P:161.976 MHz, ^{11}B: 128.378 MHz, ^{13}C{^{1}H}: 100.623 MHz) with δ [ppm] referenced to external SiMe$_4$ (^{1}H, ^{13}C), H$_3$PO$_4$ (^{31}P), and BF$_3$·Et$_2$O (^{11}B). The IR spectra were measured on a DIGILAB (FTS 800) FT-IR spectrometer (Digilab Inc., Marlborough, MA, USA) and on a Thermo Scientific Nicolet iS5 (Thermo Fisher Scientific Inc., Madison, WI, USA). The mass spectra were recorded on a Micromass LCT ESI-TOF (Waters Corporation, Wexford, Ireland) and a Jeol AccuTOF GCX (LIFDI) (JEOL Ltd., Tokyo, Japan). Elemental analyses (C, H, N) were determined on a Vario EL III instrument (Elementar Analysensysteme GmbH, Donaustraße 7, 63452 Hanau, Germany).

3.2. Synthesis and Characterization of Compounds **2**–**10**

3.2.1. Synthesis and Characterization of **2**

To a stirred solution of 365 mg tBuPHBH$_2$NMe$_3$ (2.28 mmol) in 15 mL toluene, 0.3 mL MeI (3.32 mmol) was added at room temperature. A white solid precipitated immediately. The solution was stirred for 20 h, then the supernatant was decanted, and the remaining solid was washed with 30 mL n-hexane. The solid was dissolved in a THF/MeCN (5:1) solution and layered with three volumes of n-hexane, from which compound 2 crystallized as colorless blocks. Yield of 2: 640 mg (93%). ^{1}H NMR (400.13 MHz, CD$_3$CN): δ[ppm] = 1.24 (d, 9H, $^3J_{HP}$ = 16 Hz, C(CH$_3$)$_3$), 1.58 (dd, 3H, $^2J_{HP}$ = 12 Hz, $^3J_{HH}$ = 6 Hz, CH$_3$), 2.15 (m, 2H, BH$_2$), 2.83 (s, 9H, N(CH$_3$)$_3$), 5.47 (m, 1H, $^1J_{PH}$ = 396 Hz, $^3J_{HH}$ = 6 Hz, PH). ^{31}P{^{1}H} NMR (161.975 MHz, CD$_3$CN): δ[ppm] = −15.70 (bq, $^1J_{PH}$ = 396 Hz). ^{31}P NMR (161.975 MHz, CD$_3$CN): δ[ppm] = −15.70 (bq, $^1J_{PB}$ = 78 Hz). ^{11}B{^{1}H} NMR (128.378 MHz, CD$_3$CN): δ[ppm] = −10.30 (d, $^1J_{BP}$ = 78 Hz). ^{11}B NMR (128.378 MHz, CD$_3$CN): δ[ppm] = −10.30 (dt, $^1J_{BP}$ = 78 Hz, $^1J_{BH}$ = 113 Hz). ^{13}C{^{1}H} NMR (100.613 MHz, CD$_3$CN): δ[ppm] = 26.24 (s, CH$_3$), 26.25 (s, C(CH$_3$)$_3$), 27.71 (d, $^1J_{CP}$ = 40 Hz, C(CH$_3$)$_3$), 54.98 (d, $^3J_{CP}$ = 6 Hz), N(CH$_3$)$_3$). IR (KBr): $\tilde{\upsilon}$/cm^{-1} = ν_{CO}: 2963 (m, C-H), 2949 (m, C-H), 2918 (w), 2863 (m), 2460 (m, P-H), 2414 (m), 2323 (m, B-H), 1481 (m), 1412 (w), 1375 (vw), 1298 (w), 1249 (w), 1192 (vw), 1165 (vw), 1142 (s), 1092 (m), 1034 (w), 1015 (w), 987 (vw), 945 (vw), 911 (w), 876 (w), 856 (m), 821 (w), 755 (vw), 702 (vw). EI-MS (CH$_3$CN): *m*/*z* (%) = 176 [(*t*Bu(Me)PHBH$_2$NMe$_3$)$^+$]. Elemental analysis, calcd. for C$_8$H$_{24}$BPNI (303.08 g/mol): C: 31.71%, H: 7.98%, N: 4.62%. Found C: 31.92%, H: 7.67%, N: 4.59%.

3.2.2. Synthesis and Characterization of **3**

To a stirred solution of 400 mg *t*BuPHBH$_2$NMe$_3$ (2.48 mmol) in 20 mL toluene, 0.3 mL *n*PrI (3.08 mmol) was added at room temperature. The solution was stirred for 20 h, after which all the volatiles were removed in vacuo, and the remaining solid was washed with 15 mL *n*-hexane. The solid was dissolved in a THF/MeCN (5:1) so-

lution and layered with three volumes of *n*-hexane, from which compound **3** crystallized as colorless prisms. Yield of **3**: 630 mg (70%). ^{1}H NMR (400.13 MHz, CD_3CN): δ[ppm] = 1.07 (td, 3H, $^{3}J_{HH}$ = 7 Hz, $^{4}J_{HH}$ = 1 Hz, CH_3), 1.27 (d, 9H, $^{3}J_{HP}$ = 16 Hz, $C(CH_3)_3$), 1.57–2.13 (m, 4H, CH_2), 2.40 (m, 2H, BH_2), 2.81 (d, 9H, $^{4}J_{HP}$ = 1 Hz, $N(CH_3)_3$), 5.29 (m, 1H, $^{1}J_{PH}$ = 380 Hz, $^{3}J_{HH}$ = 3 Hz, PH). ^{31}P{^{1}H} NMR (161.975 MHz, CD_3CN): δ[ppm] = −7.35 (bq, $^{1}J_{PH}$ = 380 Hz). ^{31}P NMR (161.975 MHz, CD_3CN): δ[ppm] = −7.35 (q, $^{1}J_{PB}$ = 73 Hz). ^{11}B{^{1}H} NMR (128.378 MHz, CD_3CN): δ[ppm] = −11.05 (d, $^{1}J_{BP}$ = 73 Hz). ^{11}B NMR (128.378 MHz, CD_3CN): δ[ppm] = −11.05 (dt, $^{1}J_{BP}$ = 73 Hz, $^{1}J_{BH}$ = 110 Hz). ^{13}C{^{1}H} NMR (100.613 MHz, CD_3CN): δ[ppm] = 14.74 (d, $^{2}J_{CP}$ = 14 Hz, CH_2), 18.02 (d, $^{1}J_{CP}$ = 35 Hz, H_2C-P), 18.28 (d, $^{3}J_{CP}$ = 4 Hz, CH_3), 25.84 (d, $^{2}J_{CP}$ = 1 Hz, $C(\underline{C}H_3)_3$), 27.75 (d, $^{1}J_{CP}$ = 38 Hz, $\underline{C}(CH_3)_3$), 54.09 (d, $^{3}J_{CP}$ = 6 Hz), $N(CH_3)_3$). IR (KBr): $\tilde{\upsilon}/cm^{-1}$ = ν_{CO}: 2994(w, C-H), 2958 (s, C-H), 2870 (m), 2736 (vw), 2452 (m, P-H), 2399 (w), 2286 (m, B-H), 1473 (s), 1417 (w), 1373 (w), 1247 (w), 1196 (vw), 1162 (w), 1138 (s), 1096 (m), 1054 (m), 1029 (w), 978 (w), 910 (vw), 861 (s), 820 (w), 771 (vw), 719 (vw). EI-MS(CH_3CN): m/z (%) = 535 [{(*t*Bu(*n*Pr)$PHBH_2NMe_3$)$_2$(I)}$^+$], 204 [(*t*Bu*n*Pr$PHBH_2NMe_3$)$^+$]. Elemental analysis, calcd. for $C_{10}H_{28}BPNI$ (331.11 g/mol): C: 36.28%, H: 8.52%, N: 4.23%. Found C: 36.05%, H: 8.33%, N: 3.99%.

3.2.3. Synthesis and Characterization of **4**

To a stirred solution of 240 mg *t*Bu$PHBH_2NMe_3$ (1.49 mmol) in 15 mL toluene, 0.075 mL (0.75 mmol) $C_3H_6Br_2$ was added at room temperature. The solution was stirred for 3 days, and a white solid precipitated. All the volatiles were removed in vacuo, and the remaining solid was washed with 15 mL toluene. The solid was dissolved in 10 mL CH_2Cl_2 and layered with four volumes of *n*-hexane, from which compound **4** crystallized as colorless plates. Yield of **4**: 155 mg (40%). ^{1}H NMR (400.13 MHz, CD_3CN): δ[ppm] = 1.29 (d, 18H, $^{3}J_{HP}$ = 16 Hz, $C(CH_3)_3$), 2.01–2.41 (m, 6H, CH_2), 2.27–2.61 (m, 4H, BH_2), 2.89 (s, 9H, $N(CH_3)_3$), 6.41 (m, 1H, $^{1}J_{PH}$ = 390 Hz, PH). ^{31}P{^{1}H} NMR (161.975 MHz, CD_3CN): δ[ppm] = −10.35 (m, br, $^{1}J_{PH}$ = 390 Hz). ^{31}P NMR (161.975 MHz, CD_3CN): δ[ppm] = −10.35 (m, br, $^{1}J_{PB}$ = 70 Hz). ^{11}B{^{1}H} NMR (128.378 MHz, CD_3CN): δ[ppm] = −10.87 (s, br). ^{11}B NMR (128.378 MHz, CD_3CN): δ[ppm] = −10.87 (s, br). ^{13}C{^{1}H} NMR (100.613 MHz, CD_3CN): δ[ppm] = 18.60 (d, $^{1}J_{CP}$ =35 Hz, H_2C-P), 21.81 (t, $^{3}J_{CP}$ = 3 Hz, CH_2), 26.84 (d, $^{2}J_{CP}$ = 1 Hz, $C(\underline{C}H_3)_3$), 28.79 (d, $^{1}J_{CP}$ = 38 Hz, $\underline{C}(CH_3)_3$), 55.12 (d, $^{3}J_{CP}$ = 6 Hz), $N(CH_3)_3$). ES-MS (CH_3CN): m/z (%) = 443 [{(Me_3NH_2BHP*t*Bu)*n*Pr(*t*Bu$PHBH_2NMe_3$)Br}$^+$], 363 [{(Me_3NH_2BPtBu)*n*Pr(*t*Bu$PHBH_2NMe_3$)(Br)}$^+$], 182 [(Me_3NH_2BHP*t*Bu)*n*Pr(*t*Bu$PHBH_2$-NMe_3)$^{2+}$].

3.2.4. Synthesis and Characterization of **5**

To a solution of 528 mg **2** (3.00 mmol) in 25 mL CH_3CN, 120 mg (2.99 mmol) KH were added as a solid at −40 °C. The solution was stirred at −40 °C until all the solid disappeared. All the volatiles were removed in vacuo, and the remaining white solid was dissolved in 20 mL *n*-hexane. After filtration over diatomaceous earth, the solvent was concentrated until saturation in vacuo and stored at −30 °C, from which compound **5** crystallized as colorless blocks. Yield of **5**: 287 mg (55%). ^{1}H NMR (400.13 MHz, C_6D_6): δ[ppm] = 1.34 (s, br, 3H, CH_3), 1.38 (d, 9H, $^{3}J_{HP}$ = 11 Hz, $C(CH_3)_3$), 1.95 (s, 9H, $N(CH_3)_3$), 2.45 (m, 2H, BH_2). ^{31}P{^{1}H} NMR (161.975 MHz, C_6D_6): δ[ppm] = −53.38 (q, br, $^{1}J_{PB}$ = 53 Hz). ^{31}P NMR (161.975 MHz, C_6D_6): δ[ppm] = −53.38 (m, br). ^{11}B{^{1}H} NMR (128.378 MHz, C_6D_6): δ[ppm] = −1.58 (d, $^{1}J_{BP}$ = 53 Hz). ^{11}B NMR (128.378 MHz, C_6D_6): δ[ppm] = −1.58 (dt, $^{1}J_{BP}$ = 53 Hz, $^{1}J_{BH}$ = 102 Hz). ^{13}C{^{1}H} NMR (100.613 MHz, C_6D_6): δ[ppm] = 8.40 (d, $^{1}J_{CP}$ = 17 Hz, CH_3), 26.80 (d, $^{3}J_{CP}$ = 5 Hz, $C(\underline{C}H_3)_3$), 29.41 (d, $^{2}J_{CP}$ = 5 Hz, $\underline{C}(CH_3)_3$), 52.05 (d, $^{3}J_{CP}$ = 12 Hz), $N(CH_3)_3$). IR (KBr): $\tilde{\upsilon}/cm^{-1}$ = ν_{CO}: 2941 (m, C-H), 2897 (m, C-H),

2854 (m), 2374 (m, B-H), 2288 (w), 2187 (vw), 1653 (vw), 1485 (m), 1460 (m), 1422 (w), 1400 (w), 1383 (w), 1356 (w), 1253 (w), 1187 (vw), 1152 (w), 1123 (m), 1069 (s), 1014 (w), vw), 954 (vw), 884 (vw), 868 (vw), 842 (s), 817 (w), 681 (w), 637 (vw), 581 (vw), 472 (vw). LIFDI-MS (toluene): m/z (%) = 524 [{$Me_3N(H_2BPMetBu)_4$}$^+$], 408 [{$Me_3N(H_2BPMetBu)_3$}$^+$]. Elemental analysis, calcd. for $C_8H_{23}BPN$ (175.17 g/mol): C: 54.80%, H: 13.23%, N: 7.99%. Found C: 54.66%, H: 12.90%, N: 7.90%.

3.2.5. Synthesis and Characterization of **6**

To a solution of 612 mg **3** (3.00 mmol) in 25 mL CH_3CN, 120 mg (2.99 mmol) KH were added as a solid at −40 °C. The solution was stirred at −40 °C until all the solids almost disappeared. All the volatiles were removed in vacuo, and the remaining white solid was dissolved in 20 mL *n*-hexane. After filtration over diatomaceous earth, the solvent was removed in vacuo. Compound **6** was isolated as a white solid, which was a bit waxy at room temperature. Yield of **6**: (38%, based on ^{31}P NMR). ^{1}H NMR (400.13 MHz, C_6D_6): δ[ppm] = 1.04 (t, 3H, $^3J_{HH}$ = 7 Hz, $^4J_{HH}$ = 1 Hz, CH_3), 1.37 (d, 9H, $^3J_{HP}$ = 11 Hz, $C(CH_3)_3$), 1.35–1.44 (m, 4H, CH_2), 2.38 (m, 2H, BH_2), 2.01 (s, 9H, $N(CH_3)_3$). ^{31}P{^{1}H} NMR (161.975 MHz, C_6D_6): δ[ppm] = −36.19 (bd, br, $^1J_{PH}$ = 162 Hz). ^{31}P NMR (161.975 MHz, C_6D_6): δ[ppm] = −36.21 (bd, $^1J_{PB}$ = 79 Hz). ^{11}B{^{1}H} NMR (128.378 MHz, C_6D_6): δ[ppm] = −2.33 (bd, $^1J_{BP}$ = 52 Hz). ^{11}B NMR (128.378 MHz, C_6D_6): δ[ppm] = −2.53 (m, $^1J_{BP}$ = 52 Hz, $^1J_{BH}$ = 88 Hz). Note: signals corresponding to impurities were observed in the NMR spectra (see Figures S25–S29 in the ESI).

3.2.6. Synthesis and Characterization of **7**

To a solution of 507 mg **4** (1.50 mmol) in 25 mL CH_3CN, 120 mg (2.99 mmol) KH were added as a solid at −40 °C. The solution was stirred at −40 °C until all the solids almost disappeared. All the volatiles were removed in vacuo, and the remaining white solid was dissolved in 20 mL *n*-hexane. After filtration over diatomaceous earth, the solvent was removed in vacuo. Compound **7** was isolated as a white solid, which was a bit waxy at room temperature. Yield of **7**: (24%, based on ^{31}P NMR). ^{1}H NMR (400.13 MHz, C_6D_6): δ[ppm] = 1.22 (d, 18H, $^3J_{HP}$ = 13 Hz, $C(CH_3)_3$), 1.41–1.45 (m, 6H, CH_2), 2.15–2.91 (m, 4H, BH_2), 2.26 (s, 9H, $N(CH_3)_3$). ^{31}P{^{1}H} NMR (161.975 MHz, C_6D_6): δ[ppm] = −35.77 (bd, $^1J_{PB}$ = 161 Hz). ^{31}P NMR (161.975 MHz, C_6D_6): δ[ppm] = −35.56 (bd, $^1J_{PB}$ = 160 Hz). ^{11}B{^{1}H} NMR (128.378 MHz, C_6D_6): δ[ppm] = −2.87 (s, br). ^{11}B NMR (128.378 MHz, C_6D_6): δ[ppm] = −2.66 (s, br). Note: signals corresponding to impurities were observed in the NMR spectra (see Figures S30–S34 in the ESI).

3.2.7. Synthesis and Characterization of **8**

To a solution of 120 mg (0.59 mmol) $LiPCy_2$ in 10 mL THF, a solution of 100 mg (0.50 mmol) IBH_2NMe_3 in 10 mL THF was added at −80 °C. The color of the solution changed from yellow to colorless, and the solution was allowed to reach room temperature over 18 h. All the volatiles were removed in vacuo. The remaining solid was suspended in 10 mL *n*-hexane and filtrated over diatomaceous earth. The volume was reduced to 3 mL. Compound **8** crystallized as colorless plates upon storing a saturated solution of *n*-hexane at −30 °C. Due to the similar solubility of the decomposition products of **8**, it was not possible to obtain analytically pure compound **8** (see Figures S35–S37). Yield of **8**: (30%, based on ^{31}P NMR). ^{31}P NMR (161.975 MHz, C_6D_6 capillary in THF): δ[ppm] = −37.29 (m, br). ^{11}B{^{1}H} NMR (128.378 MHz, C_6D_6 capillary in THF): δ[ppm] = −4.25 (m, br, $\omega_{1/2}$ = 200 Hz). ^{11}B NMR (128.378 MHz, C_6D_6 capillary in THF): δ[ppm] = −4.25 (m, br, $\omega_{1/2}$ = 350 Hz).

3.2.8. Synthesis and Characterization of **9**

To a solution of 304 mg (2.00 mmol) $LiPtBu_2$ in 10 mL THF, a solution of 388 mg (1.95 mmol) IBH_2NMe_3 in 10 mL THF was added at −80 °C. The color of the solution changed from yellow to colorless, and the solution was allowed to reach room temperature over 18 h. All the volatiles were removed in vacuo. The remaining white solid was suspended in 45 mL *n*-pentane and filtrated over diatomaceous earth. Compound **9** crystallized as colorless blocks upon storing a saturated solution in *n*-pentane at −30 °C. Due to the similar solubility of decomposition products of **9**, it was not possible to obtain analytically pure compound **9** (see Figures S38–S41). Compound **9** crystallized as colorless plates. Yield of **9**: (55%, based on ^{31}P NMR). ^1H NMR (400.13 MHz, C_6D_6): δ[ppm] = 1.21 (m, br, 2H, BH_2), 1.50 (d, 18H, $^3J_{HP}$ = 11 Hz, $C(CH_3)_3$), 1.96 (s, 9H, $N(CH_3)_3$). $^{31}P\{^1H\}$ NMR (161.975 MHz, C_6D_6): δ[ppm] = 8.92 (q, br, $^1J_{BP}$ = 60 Hz). ^{31}P NMR (161.975 MHz, C_6D_6): δ[ppm] = 8.92 (m, br). $^{11}B\{^1H\}$ NMR (128.378 MHz, C_6D_6): δ[ppm] = −4.18 (d, $^1J_{BP}$ = 60 Hz). ^{11}B NMR (128.378 MHz, C_6D_6): δ[ppm] = −4.18 (m, $^1J_{BP}$ = 60 Hz, $^1J_{BH}$ = 106 Hz).

3.2.9. Synthesis and Characterization of **10**

To a solution of 204 mg (1.00 mmol) $LiPCy_2$ in 10 mL THF 1 mL, a 1 M solution of IBH_2SMe_2 in toluene was added at −80 °C. The solution was allowed to reach room temperature over 18 h, and the color changed from yellow to colorless. All the volatiles were removed in vacuo, and the remaining white solid was dried for 60 min. The solid was suspended in 20 mL *n*-hexane and filtrated over diatomaceous earth. All the volatiles were removed, and the remaining solid was dried under a vacuum. Compound **10** crystallized as colorless needles upon storing a saturated solution in toluene at −30 °C. Yield of **10**: 200 mg (50%). ^1H NMR (400.13 MHz, C_6D_6): δ[ppm] = 1.06–2.36 (m, 44H, Cy), 1.90 (m, 4H, BH_2). $^{31}P\{^1H\}$ NMR (161.975 MHz, C_6D_6): δ[ppm] = −10.88 (s, br). ^{31}P NMR (161.975 MHz, C_6D_6): δ[ppm] = −10.92 (s, br). $^{11}B\{^1H\}$ NMR (128.378 MHz, C_6D_6): δ[ppm] = −3.34 (m, br). ^{11}B NMR (128.378 MHz, C_6D_6): δ[ppm] = −3.34 (m, br). LIFDI-MS (toluene): m/z (%) = 420 [$((Cy_2PBH_2)_2)^+$]. Elemental analysis, calcd. for $C_{24}H_{48}B_2P_2$ (420.34 g/mol): C: 68.51%, H: 11.24%. Found C: 68.04%, H: 11.24%.

4. Conclusions

In summary, our approach towards the alkylation of phosphanylboranes was extended to dialkylated phosphanylboranes using a similar strategy through phosphonium salt intermediates. The phosphonium salts, as well as the formed products, were all obtained as racemic mixtures of chiral compounds due to the presence of chiral P centers. The developed process may allow high flexibility in synthesizing phosphanylboranes with selected but different alkyl groups on the P atoms. These compounds could be used as potential ligands for catalytic processes, as it is well known for phosphines in general. Further, we synthesized dialkylated phosphanylboranes possessing similar alkyl groups on the P atoms from a salt metathesis reaction of $LiP(alkyl)_2$ (alkyl = *t*Bu, cyclohexyl) with $IH_2B{\bullet}LB$ (LB = NMe_3, SMe_2). Although some of the isolated compounds contain impurities arising from similar solubilities, these synthetic pathways are still generally worth extending to phosphanylboranes with a large variety of substituents and to investigate their limitations as the resulting products cannot, until today, be accessed by other methods.

Supplementary Materials: The following supporting information can be downloaded at: https://www.mdpi.com/article/10.3390/inorganics13070239/s1, Figure S1: ^1H NMR spectrum of **2**, Figure S2: $^{31}P\{^1H\}$ NMR spectrum of **2**, Figure S3: ^{31}P NMR spectrum of **2**, Figure S4: $^{11}B\{^1H\}$ NMR spectrum of **2**, Figure S5: ^{11}B NMR spectrum of **2**, Figure S6: $^{13}C\{^1H\}$ NMR spectrum of **2**, Figure S7: ^1H NMR spectrum of **3**, Figure S8: $^{31}P\{^1H\}$ NMR spectrum of **3**, Figure S9: ^{31}P NMR spec-

trum of **3**, Figure S10: $^{11}B\{^{1}H\}$ NMR spectrum of **3**, Figure S11: ^{11}B NMR spectrum of **3**, Figure S12: $^{13}C\{^{1}H\}$ NMR spectrum of **3**, Figure S13: ^{1}H NMR spectrum of **4**, Figure S14: ^{31}P NMR spectrum of **4**, Figure S15: $^{31}P\{^{1}H\}$ NMR spectrum of **4**, Figure S16: $^{11}B\{^{1}H\}$ NMR spectrum of **4**, Figure S17: ^{11}B NMR spectrum of **4**, Figure S18: $^{13}C\{^{1}H\}$ NMR spectrum of **4**, Figure S19: ^{1}H NMR spectrum of **5**, Figure S20: $^{31}P\{^{1}H\}$ NMR spectrum of **5**, Figure S21: ^{31}P NMR spectrum of **5**, Figure S22: $^{11}B\{^{1}H\}$ NMR spectrum of **5**, Figure S23: ^{11}B NMR spectrum of **5**, Figure S24: $^{13}C\{^{1}H\}$ NMR spectrum of **5**, Figure S25: ^{1}H NMR spectrum of **6**, Figure S26: $^{31}P\{^{1}H\}$ NMR spectrum of **6**, Figure S27: ^{31}P NMR spectrum of **6**, Figure S28: $^{11}B\{^{1}H\}$ NMR spectrum of **6**, Figure S29: ^{11}B NMR spectrum of **6**, Figure S30: ^{1}H NMR spectrum of **7**, Figure S31: $^{31}P\{^{1}H\}$ NMR spectrum of **7**, Figure S32: ^{31}P NMR spectrum of **7**, Figure S33: $^{11}B\{^{1}H\}$ NMR spectrum of **7**, Figure S34: ^{11}B NMR spectrum of **7**, Figure S35: ^{31}P NMR spectrum of **8**, Figure S36: ^{11}B NMR spectrum of **8**, Figure S37: $^{11}B\{^{1}H\}$ NMR spectrum of **8**, Figure S38: ^{1}H NMR spectrum of **9**, Figure S39: ^{11}B NMR spectrum of **9**, Figure S40: $^{11}B\{^{1}H\}$ NMR spectrum of **9**, Figure S41: ^{31}P NMR spectrum of **9**, Figure S42: $^{31}P\{^{1}H\}$ NMR spectrum of **9**, Figure S43: ^{1}H NMR spectrum of **10**, Figure S44: ^{11}B NMR spectrum of **10**, Figure S45: $^{11}B\{^{1}H\}$ NMR spectrum of **10**, Figure S46: ^{31}P NMR spectrum of **10**, Figure S47: $^{31}P\{^{1}H\}$ NMR spectrum of **10**, Figure S48: Molecular structure of **2** in the solid state. Thermal ellipsoids are drawn with 50% probability. Counter-anions are omitted for clarity. Figure S49: View of the asymmetric unit of **3** in the solid state. Thermal ellipsoids are drawn with 50% probability. Counter-anions are omitted for clarity. Figure S50: Molecular structure of **4** in the solid state. Thermal ellipsoids are drawn with 50% probability. Counter-anions are omitted for clarity. Figure S51: Molecular structure of **5** in the solid state. Thermal ellipsoids are drawn with 50% probability. Counter-anions are omitted for clarity. Figure S52: Molecular structure of **8** in the solid state. Thermal ellipsoids are drawn with 50% probability. Counter-anions are omitted for clarity. Figure S53: Molecular structure of **9** in the solid state. Thermal ellipsoids are drawn with 50% probability. Counter-anions are omitted for clarity. Figure S54: Molecular structure of **10** in the solid state. Thermal ellipsoids are drawn with 50% probability. Counter-anions are omitted for clarity. Table S1: Crystallographic data for compounds **2–5**, Table S2: Crystallographic data for compounds **8–10**. References [54–57] are cited in the supplementary materials.

Author Contributions: Synthesis and characterization of compounds **6** and **7**, literature study, and manuscript preparation, M.E.M.; synthesis of all other compounds and their characterizations, O.H.; preparation of final CIF files for all compounds and revising the X-ray part, C.R.; correction of and finalizing the manuscript, supervision of the whole project, and funding acquisition, M.S. All authors have read and agreed to the published version of the manuscript.

Funding: This work was financially supported by the Deutsche Forschungsgemeinschaft within the project Sche 384/41-2.

Institutional Review Board Statement: Not applicable.

Informed Consent Statement: Not applicable.

Data Availability Statement: NMR spectra and crystal data are given in the Supporting Information. Crystallographic data for compounds **2–10** have been deposited with the Cambridge Crystallographic Data Center (CCDC 2464405-2464411).

Acknowledgments: The authors thank the Deutsche Forschungsgemeinschaft for the support within the project Sche 384/41-2. C.R. is grateful for the Studienstiftung des Deutschen Volkes e. V. for his PhD fellowship.

Conflicts of Interest: The authors declare no conflicts of interest.

References

1. Wiebe, M.A.; Staubitz, A.; Manners, I. Dehydrocoupling of Phosphine-Borane Adducts Under Ambient Conditions Using Aminoboranes as Hydrogen Acceptors. *Chem. Eur. J.* **2025**, *31*, e202403849. [CrossRef] [PubMed]
2. Gayen, S.; Ghosh, S. Recent Advances of B−P Coupling Reactions: Conventional and Efficient Alternative Routes. *Eur. J. Inorg. Chem.* **2025**, *28*, e202400732. [CrossRef]

3. Race, J.J.; Heyam, A.; Wiebe, M.A.; Hernandez, J.D.-G.; Ellis, C.E.; Lei, S.; Manners, I.; Weller, A.S. Polyphosphinoborane Block Copolymer Synthesis Using Catalytic Reversible Chain-Transfer Dehydropolymerization. *Angew. Chem. Int. Ed.* **2023**, *62*, e202216106. [CrossRef] [PubMed]
4. Oldroyd, N.L.; Chitnis, S.S.; Annibale, V.T.; Arz, M.I.; Sparkes, H.A.; Manners, I. Metal-free dehydropolymerisation of phosphine-boranes using cyclic (alkyl)(amino)carbenes as hydrogen acceptors. *Nat. Commun.* **2019**, *10*, 1370. [CrossRef]
5. Turner, J.R.; Resendiz-Lara, D.A.; Jurca, T.; Schäfer, A.; Vance, J.R.; Beckett, L.; Whittell, G.R.; Musgrave, R.A.; Sparkes, H.A.; Manners, I. Synthesis, Characterization, and Properties of Poly(aryl)phosphinoboranes Formed via Iron-Catalyzed Dehydropolymerization. *Macromol. Chem. Phys.* **2017**, *218*, 1700120. [CrossRef]
6. Schäfer, A.; Jurca, T.; Turner, J.; Vance, J.R.; Lee, K.; Du, V.A.; Haddow, M.F.; Whittell, G.R.; Manners, I. Iron-Catalyzed Dehydropolymerization: A Convenient Route to Poly(phosphinoboranes) with Molecular-Weight Control. *Angew. Chem. Int. Ed.* **2015**, *54*, 4836–4841. [CrossRef]
7. Pandey, S.; Lönnecke, P.; Hawkins, E.H. Phosphorus–Boron-Based Polymers Obtained by Dehydrocoupling of Ferrocenylphosphine–Borane Adducts. *Eur. J. Inorg. Chem.* **2014**, *2014*, 2456–2465. [CrossRef]
8. Clark, T.L.; Rodezno, J.M.; Clendenning, S.B.; Aouba, S.; Brodersen, P.M.; Lough, A.J.; Ruda, H.E.; Manners, I. Rhodium-Catalyzed Dehydrocoupling of Fluorinated Phosphine–Borane Adducts: Synthesis, Characterization, and Properties of Cyclic and Polymeric Phosphinoboranes with Electron-Withdrawing Substituents at Phosphorus. *Chem. Eur. J.* **2005**, *11*, 4526–4534. [CrossRef]
9. Dorn, H.; Rodenzo, J.M.; Brunnhöfer, B.; Rivard, E.; Massey, J.A.; Manners, I. Synthesis, Characterization, and Properties of the Polyphosphinoboranes $[RPH-BH_2]_n$ (R = Ph, *i*Bu, *p*-*n*BuC_6H_4, *p*-dodecylC_6H_4): Inorganic Polymers with a Phosphorus−Boron Backbone. *Macromolecules* **2003**, *36*, 291–297. [CrossRef]
10. Burg, A.B.; Wagner, R.I. Chemistry of P-B Bonding: The Phosphinoborines and Their Polymers. *J. Am. Chem. Soc.* **1953**, *75*, 3872–3877. [CrossRef]
11. Onodera, G.; Kumagae, H.; Nakamura, D.; Hayasaki, T.; Fukuda, T.; Kimura, M. Direct benzylation of amines with benzylic alcohols catalyzed by palladium/phosphine-borane catalyst system. *Tetrahedron Lett.* **2020**, *61*, 152537. [CrossRef]
12. Morris, L.J.; Hill, M.S.; Mahon, M.F.; Manners, I.; Patrick, B.O. Alkaline-Earth Derivatives of Diphenylphosphine–Borane. *Organometallics* **2020**, *39*, 4195–4207. [CrossRef]
13. Bas de Jong, G.; Ortega, N.; Lutz, M.; Lammertsma, K.; Slootweg, J.C. Easy Access to Phosphine-Borane Building Blocks. *Chem. Eur. J.* **2020**, *26*, 15944. [CrossRef] [PubMed]
14. Lemouzy, S.; Membrat, R.; Oliviere, E.; Jean, M.; Albalat, M.; Nuel, D.; Giordano, L.; Hérault, D.; Buono, G. Umpolung Reactivity of in Situ Generated Phosphido-Boranes: An Entry to P-Stereogenic Aminophosphine-Boranes. *J. Org. Chem.* **2019**, *84*, 4551–4557. [CrossRef]
15. Konishi, S.; Iwai, T.; Sawamura, M. Synthesis, Properties, and Catalytic Application of a Triptycene-Type Borate-Phosphine Ligand. *Organometallics* **2018**, *37*, 1876–1883. [CrossRef]
16. Dutartre, M.; Bayardon, J.; Jugé, S. Applications and stereoselective syntheses of P-chirogenic phosphorus compounds. *Chem. Soc. Rev.* **2016**, *45*, 5771–5794. [CrossRef]
17. Alayrac, C.; Lakhdar, S.; Abdellah, I.; Gaumont, A.-C. Recent Advances in Synthesis of P-BH_3 Compounds. *Top. Curr. Chem.* **2014**, *361*, 1. [CrossRef]
18. Amgoune, A.; Bouhadir, G.; Bourissou, D. Reactions of Phosphine-Boranes and Related Frustrated Lewis Pairs with Transition Metal Complexes. *Top. Curr. Chem.* **2013**, *334*, 281. [CrossRef]
19. Imamoto, T.; Tamura, K.; Zhang, Z.; Horiuchi, Y.; Sugiya, M.; Yoshida, K.; Yanagisawa, A.; Grindnev, I.D. Rigid P-Chiral Phosphine Ligands with *tert*-Butylmethylphosphino Groups for Rhodium-Catalyzed Asymmetric Hydrogenation of Functionalized Alkenes. *J. Am. Chem. Soc.* **2012**, *134*, 1754–1769. [CrossRef]
20. Consiglio, G.B.; Queval, P.; Harrison-Marchand, A.; Mordini, A.; Lohier, J.-F.; Delacroix, O.; Gaumont, A.-C.; Gérard, H.; Maddaluno, J.; Oulyadi, H. $Ph_2P(BH_3)Li$: From Ditopicity to Dual Reactivity. *J. Am. Chem. Soc.* **2011**, *133*, 6472–6480. [CrossRef]
21. Geier, S.J.; Gilbert, T.M.; Stephan, D.W. Synthesis and Reactivity of the Phosphinoboranes $R_2PB(C_6F_5)_2$. *Inorg. Chem.* **2011**, *50*, 336–344. [CrossRef]
22. Staubitz, A.; Robertson, A.P.M.; Sloan, M.E.; Manners, I. Amine− and Phosphine−Borane Adducts: New Interest in Old Molecules. *Chem. Rev.* **2010**, *110*, 4023–4078. [CrossRef] [PubMed]
23. Janus, D.A.; Lieven, C.J.; Crowe, M.E.; Levin, L.A. Polyester-based microdisc systems for sustained release of neuroprotective phosphine-borane complexes. *Pharm. Dev. Technol.* **2018**, *23*, 882–889. [CrossRef]
24. Niemuth, N.J.; Thompson, A.F.; Crowe, M.E.; Lieven, C.J.; Levin, L.A. Intracellular disulfide reduction by phosphine-borane complexes: Mechanism of action for neuroprotection. *Neurochem. Int.* **2016**, *99*, 24–32. [CrossRef] [PubMed]
25. Crowe, M.E.; Lieven, C.J.; Thompson, A.F.; Sheibani, N.; Levin, L.A. Borane-protected phosphines are redox-active radioprotective agents for endothelial cells. *Redox Biol.* **2015**, *6*, 73–79. [CrossRef] [PubMed]
26. LaFortune, J.H.W.; Qu, Z.-W.; Bamford, K.L.; Trofimova, A.; Westcott, S.A.; Stephan, D.W. Double Phosphinoboration of CO_2: A Facile Route to Diphospha-Ureas. *Chem. Eur. J.* **2019**, *25*, 12063–12067. [CrossRef]

27. Szynkiewicz, N.; Ordyszewska, A.; Chojnacki, J.; Grubba, R. Diaminophosphinoboranes: Effective reagents for phosphinoboration of CO_2. *RSC Adv.* **2019**, *9*, 27749–27753. [CrossRef]
28. Courtemanche, M.-A.; Légaré, M.-A.; Maron, L.; Fontaine, F.-G. A Highly Active Phosphine–Borane Organocatalyst for the Reduction of CO_2 to Methanol Using Hydroboranes. *J. Am. Chem. Soc.* **2013**, *135*, 9326–9329. [CrossRef]
29. Geier, S.J.; Gilbert, T.M.; Stephan, D.W. Activation of H_2 by Phosphinoboranes $R_2PB(C_6F_5)_2$. *J. Am. Chem. Soc.* **2008**, *130*, 12632–12633. [CrossRef]
30. Welch, G.C.; Juan, R.R.S.; Masuda, J.D.; Stephan, D.W. Reversible, Metal-Free Hydrogen Activation. *Science* **2006**, *314*, 1124–1126. [CrossRef]
31. Brunel, J.M.; Faure, B.; Maffei, M. Phosphane–boranes: Synthesis, characterization and synthetic applications. *Coord. Chem. Rev.* **1998**, *178–180*, 665–698. [CrossRef]
32. Yamada, M.; Goto, M.; Yamano, M. Direct conversion of *sec*-phosphine oxides to *sec*-phosphine-boranes using BH_3. *Tetrahedron Lett.* **2021**, *67*, 152837. [CrossRef]
33. Xiao, Y.; Yang, X.; Li, H.; Yin, Y.; Du, J.; Liang, J.; Duan, W.; Yu, L. Palladium-Catalyzed Coupling of Aryl Chlorides with Secondary Phosphines to Construct Unsymmetrical Tertiary Phosphines. *Tetrahedron* **2021**, *86*, 10564–10569. [CrossRef]
34. Marquardt, C.; Adolf, A.; Stauber, A.; Bodensteiner, M.; Virovets, A.V.; Timoshkin, A.; Scheer, M. The Lewis Base Stabilized Parent Arsanylborane $H_2AsBH_2{\cdot}NMe_3$. *Angew. Chem. Int. Ed.* **2013**, *19*, 11887–11891. [CrossRef]
35. Schwan, K.-C.; Timoshkin, A.; Zabel, M.; Scheer, M. Lewis Base Stabilized Phosphanylborane. *Chem. Eur. J.* **2006**, *12*, 4900–4908. [CrossRef]
36. Braese, J.; Schinabeck, A.; Bodensteiner, M.; Yersin, H.; Timoshkin, A.Y.; Scheer, M. Gold(I) Complexes Containing Phosphanyl- and Arsanylborane Ligands. *Chem. Eur. J.* **2018**, *24*, 10073–10077. [CrossRef] [PubMed]
37. Marquardt, C.; Hegen, O.; Kahoun, T.; Scheer, M. Oxidation of Substituted Phosphanylboranes with Chalcogens. *Chem. Eur. J.* **2017**, *23*, 4397–4404. [CrossRef]
38. Thoms, C.; Marquardt, C.; Timoshkin, A.Y.; Bodensteiner, M.; Scheer, M. The Oligomerization of Phosphinoborane by Titanium Complexes. *Angew. Chem. Int. Ed.* **2013**, *52*, 5150–5154. [CrossRef]
39. Marquardt, C.; Jurca, T.; Schwan, K.-C.; Stuaber, A.; Virovets, A.V.; Whittell, G.R.; Manners, I.; Scheer, M. Metal-Free Addition/Head-to-Tail Polymerization of Transient Phosphinoboranes, RPH-BH_2: A Route to Poly(alkylphosphinoboranes). *Angew. Chem. Int. Ed.* **2015**, *54*, 13782–13786. [CrossRef]
40. Marquardt, C.; Kahoun, T.; Stauber, A.; Balázs, G.; Bodensteiner, M.; Timoshkin, A.Y.; Scheer, M. Anionic Chains of Parent Pnictogenylboranes. *Angew. Chem. Int. Ed.* **2016**, *55*, 14828–14832. [CrossRef] [PubMed]
41. Marquardt, C.; Thoms, C.; Stauber, A.; Balázs, G.; Bodensteiner, M.; Scheer, M. Cationic Chains of Phosphanyl- and Arsanylboranes. *Angew. Chem. Int. Ed.* **2014**, *53*, 3727–3730. [CrossRef] [PubMed]
42. Hills, I.D.; Netherton, M.R.; Fu, G.C. Toward an Improved Understanding of the Unusual Reactivity of Pd^0/Trialkylphosphane Catalysts in Cross-Couplings of Alkyl Electrophiles: Quantifying the Factors That Determine the Rate of Oxidative Addition. *Angew. Chem. Int. Ed.* **2003**, *42*, 5749–5752. [CrossRef]
43. Power, P.P. Boron-Phosphorus Compounds and Multiple Bonding. *Angew. Chem. Int. Ed.* **1990**, *29*, 449–460. [CrossRef]
44. Stauber, A.; Jurca, T.; Marquardt, C.; Fleischmann, M.; Seidl, M.; Whittell, G.R.; Manners, I.; Scheer, M. A Convenient Route to Monoalkyl-Substituted Phosphanylboranes (HRP–BH2–NMe_3): Prospective Precursors to Poly[(alkylphosphino)boranes]. *Eur. J. Inorg. Chem.* **2016**, *2016*, 2684–2687. [CrossRef]
45. Lehnfeld, F.; Oswald, T.; Beckhaus, R.; Scheer, M. Mono-Alkyl-Substituted Phosphinoboranes (HRP–BH_2–NMe_3) as Precursors for Poly(alkylphosphinoborane)s: Improved Synthesis and Comparative Study. *Inorganics* **2023**, *11*, 377. [CrossRef]
46. Kuzu, M.Y.; Schmidt, A.; Strohmann, C. Enantioselective Synthesis of Phosphine Boranes via Crystallization-Induced Dynamic Resolution of Lithiated Intermediate by Understanding the Underlying Epimerization Process. *Angew. Chem. Int. Ed.* **2024**, *63*, e202319665. [CrossRef]
47. Headley, C.E.; Marsden, S.P. Synthesis and Application of *P*-Stereogenic Phosphines as Superior Reagents in the Asymmetric Aza-Wittig Reaction. *J. Org. Chem.* **2007**, *72*, 7185. [CrossRef]
48. Vedejs, E.; Jure, M. Efficiency in Nonenzymatic Kinetic Resolution. *Angew. Chem. Int. Ed.* **2005**, *44*, 3974–4001. [CrossRef]
49. Williams, B.S.; Dani, P.; Lutz, M.; Spek, A.L.; van Koten, G. Development of the First P-Stereogenic PCP Pincer Ligands, Their Metallation by Palladium and Platinum, and Preliminary Catalysis. *Helv. Chim. Acta* **2001**, *84*, 3519–3530. [CrossRef]
50. Vedej, E.; Donde, Y. Stereogenic P-Trisubstituted Phosphorus by Crystallization-Induced Asymmetric Transformation: A Practical Synthesis of Phenyl(o-anisyl)methylphosphine Borane. *J. Am. Chem. Soc.* **1997**, *119*, 9293–9294. [CrossRef]
51. Tam, E.C.Y.; Maynard, N.A.; Apperley, D.C.; Smith, J.D.; Coles, M.P.; Fulton, J.R. Group 14 Metal Terminal Phosphides: Correlating Structure with $|J_{MP}|$. *Inorg. Chem.* **2012**, *51*, 9403–9415. [CrossRef] [PubMed]
52. Marquardt, C.; Hegen, O.; Hautmann, M.; Balázs, G.; Bodensteiner, M.; Virovets, A.V.; Timoshkin, A.Y.; Scheer, M. Isolation and Characterization of Lewis Base Stabilized Monomeric Parent Stibanylboranes. *Angew. Chem. Int. Ed.* **2015**, *127*, 13122–13125. [CrossRef] [PubMed]

53. Bondi, A. van der Waals Volumes and Radii. *J. Phys. Chem.* **1964**, *68*, 441. [CrossRef]
54. Agilent. *CrysAlisPro 2014*; Agilent Technologies Ltd.: Yarnton, UK, 2014.
55. Dolomanov, O.V.; Bourhis, L.J.; Gildea, R.J.; Howard, J.A.K.; Puschmann, H. OLEX2: A Complete Structure Solution, Refinement and Analysis Program. *J. Appl. Crystallogr.* **2009**, *42*, 339–341. [CrossRef]
56. Sheldrick, G.M. SHELXT-Integrated Space-Group and Crystal-Structure Determination. *Acta Crystallogr. Sect. A* **2015**, *A71*, 3–8. [CrossRef] [PubMed]
57. Sheldrick, G.M. Crystal Structure Refinement with SHELXL. *Acta Crystallogr. C* **2015**, *C71*, 3–8. [CrossRef]

Disclaimer/Publisher's Note: The statements, opinions and data contained in all publications are solely those of the individual author(s) and contributor(s) and not of MDPI and/or the editor(s). MDPI and/or the editor(s) disclaim responsibility for any injury to people or property resulting from any ideas, methods, instructions or products referred to in the content.